A pre-monsoon signal of false alarms of Indian monsoon droughts

Bidyut Bikash Goswami[1]

[1]Institute of Science and Technology, Austria.

Key Points:

- Pre-monsoon rainfall over northeastern India is a potential indicator of false alarms of monsoon drought over central Indian region
- Association between northeastern India pre-monsoon rainfall and monsoon rainfall over central India oscillates multidecadally
- Sea surface temperature anomalies in the Pacific are a key driver of pre-monsoon rainfall over the northeastern India

Corresponding author: Bidyut Bikash Goswami, `bgoswami@ista.ac.at`

Abstract

Current knowledge suggests a drought Indian monsoon (perhaps a severe one) when the El Nino Southern Oscillation and Pacific Decadal Oscillation each exhibit positive phases (a joint positive phase). For the monsoons, which are exceptions in this regard, we found northeast India often gets excess pre-monsoon rainfall. Further investigation reveals that this excess pre-monsoon rainfall is produced by the interaction of the large-scale circulation associated with the joint phase with the mountains in northeast India. We posit that a warmer troposphere, a consequence of excess rainfall over northeast India, drives a stronger monsoon circulation and enhances monsoon rainfall over central India. Hence, we argue that pre-monsoon rainfall over northeast India can be used for seasonal monsoon rainfall prediction over central India. Most importantly, its predictive value is at its peak when the Pacific Ocean exhibits a joint positive phase and the threat of extreme drought monsoon looms over India.

Plain Language Summary

Monsoon brings rain over India. But some years are droughts. These drought monsoon years are historically associated with warmer sea surface temperatures (SST) in the eastern Pacific and cooler SST in the northern Pacific. This motivated scientists to predict drought monsoons when we observe a warm eastern and cold northern Pacific Ocean. However, in some years, the monsoon is not drought despite the SST anomalies in the Pacific suggesting so. We find that, in such years, rainfall over northeastern India during pre-monsoon months is often excessive. So we argue that when the Pacific Ocean state suggests a drought monsoon over India (central region) but if pre-monsoon rainfall over northeastern India is excessive, then we can rely less on the drought signal of the Pacific Ocean.

1 Introduction

Indian Meteorology Department recently revised the normal seasonal Indian summer monsoon (ISM, or simply monsoon) mean rainfall amount. It was 880.6mm, and now it is 868.6mm (with effect from the monsoon season 2022 ("Updated Rainfall Normal based on data of 1971-2020", 2022)). Perhaps it is the simplest information to indicate that the Indian monsoon rainfall has decreased in the last half a century. The latest Intergovernmental Panel on Climate Change (IPCC) report, however, projects monsoon rain-

fall to increase in the near future (Douville et al., 2021). Reportedly, these projections are based upon the models that struggle to capture many critical aspects of the Indian monsoon (Wang et al., 2020). Nonetheless, what has been recently observed and is also widely expected and confidently projected to occur in the future, are severe droughts and floods over India (Mujumdar et al., 2020). The Indian monsoon's decreasing degree of association with El Nino Southern Oscillation (Kumar et al., 1999) further underscores the need to look for prior indicators of monsoon strength (Shahi et al., 2019; Takaya et al., 2021; Saha et al., 2021). It is noteworthy that since 1871, nearly 50% of monsoon flood and drought seasons did not follow large-scale signals from the Pacific (Singh et al., 2019). A comprehensive understanding of drivers of seasonal rainfall over India is hence much needed. A recent remarkable success was understanding such non El Nino monsoon droughts (Borah et al., 2020). We report here one pre-monsoon indicator of monsoon non-drought years, especially when it is expected, based on Pacific Ocean sea surface temperature anomalies, to be a drought.

Indian Meteorology Department's definition of normal seasonal monsoon rainfall considers rainfall over all the regions of India. Most scientific studies on monsoon, however, consider the central Indian region (B. N. Goswami, 2005) (represented by the red box in Fig. 1) to define the strength of the monsoon. It is because of the considerable homogeneity of rainfall over the central region of India. The mountains of the north, west, and northeast India, and the southern part of India, which experience the northeast monsoon, are intentionally avoided from this definition. In the rest of this paper, we shall use the words flood and drought in the context of the central Indian region unless otherwise mentioned. The Indian monsoon season typically starts in June and stays until September. The northeastern region of India (represented by the blue box in Fig. 1) is an exception (Fig. 1). While pre-monsoon rainfall over central India is merely 4.2% of its monsoon rainfall, pre-monsoon rainfall over the northeastern region is 36.2% of its monsoon rainfall (Supplementary Fig. S1). The daily mean pre-monsoon rainfall over northeast India is 6.2 mm. The northeast Indian region is climatologically very wet (Parthasarathy, 1995) (one of the wettest globally). The pre-monsoon rainfall over India is dominantly contributed by isolated afternoon convection. These rainy clouds are fueled by the heating from below by the pre-monsoon solar radiation, absorbed by the ground during the day (Thomas et al., 2018). Consequently, pre-monsoon rainfall over India exhibits a prominent preference for rainfall during the afternoon around 5:30 PM local time (Supplemen-

tary Fig. S2). Such a clear preference for rainfall timing during the day is absent over northeastern India during the pre-monsoon season. This behavior can be partially explained by the complex terrain of northeastern India which may influence the local rainfall via Katabatic winds (Ray et al., 2016). Another observation is that pre-monsoon rainfall over northeastern India (NE) occurs in long spells of decent volumes of rain (Supplementary Fig. S3), a feature commonly seen for monsoon rain over central India (CI). The rain spells over NE are much longer and more intense compared to the CI region during pre-monsoon season. These observations indicate a possibility of a large-scale driver of pre-monsoon rainfall over NE (NE_{premon}). A large-scale driver of NE_{premon} suggests a potential for seasonal prediction of monsoon rainfall over CI ($CI_{monsoon}$) if there exists a statistical relationship between NE_{premon} and $CI_{monsoon}$. With this premise, we address two specific questions in the sections to follow:

1. Is there any statistical relationship between NE_{premon} and $CI_{monsoon}$?

2. If yes, what drives NE_{premon}?

In the subsequent sections of the paper, Central India (CI) and Northeast India (NE) means the regions bounded by 18°N–28°N, 75°E–84°E, and 21.5°N–30°N, 89°E–98°E, respectively (Indicated by the red and blue boxes, respectively, in Fig. 1). The notations NE_{premon}, and $NE_{monsoon}$ mean pre-monsoon (Mar-May) and monsoon (June-Sept) seasonal mean rainfall, respectively, over NE and the same over CI are denoted by CI_{premon}, and $CI_{monsoon}$. The terms 'drought' and 'flood' are essentially defined over CI and not the whole of India, unless otherwise mentioned, for example, while carrying out the calculations for Supplementary Fig. S13). A joint positive PDO and ENSO phase is defined as more than one standard deviation of the pre-monsoon mean of PDO and ENSO multiplied index. All the correlations depicted in the study are the estimates of Pearson correlation.

2 Statistical relationship between NE_premon and CI_monsoon

Historically, monsoon rainfall over northeast India ($NE_{monsoon}$) is known to be out of phase with $CI_{monsoon}$ (Choudhury et al., 2019). Considering the period between 1901-2018, the correlation between $CI_{monsoon}$ and $NE_{monsoon}$ is -0.058. A single correlation value might be incapable of conveying a complete picture since its strength exhibits profound multi-decadal variation and becoming more and more negatively strong in the last

70 years (Supplementary Fig. S4). A comprehensive understanding of this association between $CI_{monsoon}$ and $NE_{monsoon}$ warrants further research. Our focus here is the correlation between $CI_{monsoon}$ and NE_{premon}. For the period 1901-2018, $CI_{monsoon}$ is related to pre-monsoon rainfall over NE India (NE_{premon}) with a correlation value of 0.105 (noticeably, this correlation is stronger than the $NE_{monsoon}$ and $CI_{monsoon}$ correlation). Although statistically still insignificant, a relatively stronger correlation between $CI_{monsoon}$ and NE_{premon} is intriguing.

$CI_{monsoon}$ is known to exhibit multi-decadal oscillations (L. Krishnamurthy & Krishnamurthy, 2014)(Yellow line in Fig. 2). We find that NE_{premon} also exhibits similar oscillatory behavior (Green line in Fig. 2). Since $CI_{monsoon}$ and NE_{premon}, both undergo multi-decadal oscillations, a running correlation may reveal more indicative insight about the relationship. Although not always, an 11-year running correlation is a logical option to bring out decadal/inter-decadal monsoon oscillatory behaviour (V. Krishnamurthy & Goswami, 2000). The significance and general behavior of our results do not change for a change in the length of the running correlation window, for example, from 11 to 21 years (some studies use a 21-year window (Yun & Timmermann, 2018)). An 11-year running correlation reveals that $CI_{monsoon}$ and NE_{premon} association exhibits a prominent multi-decadal variation. In the decades centered around the years 1951 and 1981 (marked by the red dotted lines in Fig. 2), the correlation is significantly positive. A careful inspection of this multi-decadal variation of the correlation strength suggests its close association with NE_{premon} as indicated by a correlation of 0.43 between the thick-black and the green lines in Fig. 2. One might argue a comparison of running mean might be inconclusive. Here, a year-to-year inspection of NE_{premon} and $CI_{monsoon}$ can shed important insight. Fig. 2 depicts that in the 118 years of IMD rainfall records analyzed, out of the 19 times NE_{premon} was excess (marked by blue circles in Fig. 2), 15 times $CI_{monsoon}$ was non-drought (marked by red circles in Fig. 2). Conversely, out of the 19 $CI_{monsoon}$ floods, only on 6 occasions NE_{premon} was a drought (Supplementary Fig. S5). During the specific periods of high correlation, indicated by the two ellipses in Fig. 2, there was only one instance, out of 13 when a drought $CI_{monsoon}$ followed an excess NE_{premon}. Intuitively, on two-thirds of the occasions, an excess NE_{premon} suggests a non-drought $CI_{monsoon}$ to follow. It provides a potential for utilizing NE_{premon} to predict the state of $CI_{monsoon}$ during decades when their correlation is significantly

139 positive. This scope hinges on the answer to the second question that we had posed ear-

140 lier, "What drives NE_{premon}?".

3 Driver of NE$_{premon}$ and causality

142   A common practice, to identify large-scale drivers of local/regional rainfall, is to

143 compute the simultaneous correlation of rainfall with sea-surface temperature (SST) glob-

144 ally. We adopted the same approach and computed correlations of NE_{premon} with mean

145 pre-monsoon SST at every grid point of the globe for the period 1901-2018. The result-

146 ing spatial correlation map (Fig. 3) resembled fairly well a familiar SST pattern that,

147 in the context of the Indian monsoon, has been reported in several earlier studies with

148 the exception that all the previous studies focused on the monsoon season (L. Krishna-

149 murthy & Krishnamurthy, 2014; Choudhury et al., 2019). Earlier studies found this SST

150 pattern to be the joint warm (or positive) phases of the Pacific Decadal Oscillation (PDO)

151 and El Nino Southern Oscillation (ENSO).

152   A joint positive PDO and positive ENSO (i.e., El Nino) phase modulates the Walker

153 and monsoon Hadley cells in ways that enhance or suppress monsoon rainfall (L. Krish-

154 namurthy & Krishnamurthy, 2014). Reportedly, monsoon and PDO are negatively re-

155 lated, and a positive PDO phase is associated with deficit monsoon rainfall (Malik et al.,

156 2017). Monsoon rainfall during El Nino years, historically, more often than not, are deficit

157 (Singh et al., 2019). A positive PDO phase, which is similar to the El Nino SST anomaly

158 pattern, that is warm SST anomalies in the eastern equatorial Pacific and cold SST anoma-

159 lies in the northern Pacific, reinforces the El Nino impact on monsoon and is expected

160 to drive more intense droughts (L. Krishnamurthy & Krishnamurthy, 2014). It is intrigu-

161 ing because we find precursors of non-drought monsoons in terms of excess pre-monsoon

162 rainfall over northeastern India for years with global SST anomalies, that resemble a joint

163 positive PDO and ENSO phase, which otherwise signals a drought monsoon. While be-

164 cause of the low frequency of PDO, knowledge of the state of PDO provides a scope of

165 long-term predictability of seasonal monsoon rainfall, we find a seasonal signal for in-

166 stances of exception to a generally expected behavior of seasonal mean monsoon strength

167 under joint positive PDO and ENSO phases.

168   Previous research finds that PDO modulates monsoon rainfall over northeastern

169 India on multidecadal time-scales (Myers et al., 2015; Choudhury et al., 2019). Choudhury

et al. (2019)'s argument was they found stronger correlation between a 7-year running mean of $NE_{monsoon}$ and northern Pacific SST than their simultaneous interannual correlation. We also found a stronger correlation between a 7-year running mean of NE_{premon} and pre-monsoon mean northern Pacific SST (Supplementary Fig. S6). However, a mechanistic understanding of this association is missing. How PDO affects the Indian monsoon is better understood (L. Krishnamurthy & Krishnamurthy, 2014) via a seasonal footprinting mechanism. Cold SST anomalies in the northern Pacific during a given winter season generate an SST footprint in the subtropics that persists into the next summer season and affects the equatorial trade winds and consequently affects the Walker and Hadley circulations impacting the Indian monsoon. This mechanism is not applicable in our study due to two reasons: 1) our results are about cases (that is, seasons) that are about non-drought years that are exceptions given cold north Pacific SST anomalies as per this mechanism; and 2) we find the maximum correlation for the current year and not with north-Pacific SST leading by one year (Supplementary Fig. S7 and S8). We shall argue that a mechanism unraveled by Sharma et al. (2023) very recently is relevant here.

We adopted a compositing approach to distill a possible mechanism. We compared a composite of 3 years of data when excess NE_{premon} was followed by above long-term average $CI_{monsoon}$ (years marked by red diamonds in Fig. 2: we call them TRUE cases) with the composite of 3 years of data when excess NE_{premon} was followed by $CI_{monsoon}$ below its long-term average (years marked by red squares in Fig. 2: we call them FALSE cases). The 6 years of data considered, TRUE and FALSE cases combined, are within the envelope of strong positive correlation between NE_{premon} and $CI_{monsoon}$ (indicated by the right-hand side ellipse in Fig. 2). We did not pick the years enveloped by the left-hand side ellipse in Fig. 2 because of the non-availability of reliable data. Arguably, an analysis based on a comparison of 3-year composites is debatable. Nevertheless, the consistency of our results with the results of Sharma et al. (2023) is intriguing. Anomalous pre-monsoon SST field, especially the cold anomalies within 145-175W and 35-48N (Supplementary Fig. S9), for TRUE composite, is expectedly similar to the correlation map depicted in Fig. 3. The associated circulation features, described below, unravel a possible causal relation between a joint positive PDO-ENSO state, NE_{premon} and $CI_{monsoon}$.

Sharma et al. (2023) found that May rainfall over NE comes from the interaction of the large-scale circulation with the local orography. The extra-tropical low-frequency

waves drive a barotropic convergence interacting with the local orography. It is noteworthy that Sharma et al. (2023)'s finding of considerable contribution from lengthy rain spells to the total May rainfall over NE (their Supplementary Fig. S12) is consistent with our Supplementary Fig. S3. We note that TRUE cases exhibit a barotropic convergence over NE India (Fig. 4), consistent with what was reported by Sharma et al. (2023). The black geopotential contours in Fig. 4 depict topography (5000 m2/s2 contour emphasized in thick magenta contour). Convergence (shaded in red) at both low and high levels is apparent in the valley region sandwiched between the mountains of NE. The 850hPa convergence confined within the thick magenta contour over NE emphasizes it. Tighter convergence drives more intense convection and latent heating (Supplementary Fig. S10). Latent heating associated with monsoon rainfall is vital to sustaining the Indian monsoon. If the latent heating associated with NE_{premon} is large enough, it can potentially impact the $CI_{monsoon}$. An indicator of this latent heating is the tropospheric temperature (Xavier et al., 2007). In the tropospheric temperature gradient definition of Xavier et al. (2007), ∇TT index, more heating associated with enhanced NE_{premon} means increased tropospheric temperature of the northern box and ∇TT may attain positive values earlier. If this happened, we should see an earlier monsoon onset for the TRUE composite. Indeed, we see an earlier onset of $CI_{monsoon}$ for the TRUE composite (Supplementary Fig. S11), according to the monsoon onset definition based on ∇TT transitioning from negative to positive values. We also note that for the TRUE composite, ∇TT total positive area-under-the-curve is more than that for the FALSE composite, consistent with a stronger monsoon. We suspect an early kick from the enhanced NE_{premon} helps sustain a stronger monsoon circulation. At this stage of our analysis, we do not have any conclusive evidence to prove it except a clue that for TRUE-composite we see positive rainfall anomalies over the central Indian region that migrates northeastwards relatively rapidly compared to the FALSE composite (Supplementary Fig. S12). Given the complex dynamics of the Indian monsoon with many remote and local drivers, our speculation needs further research, as does a marginally delayed monsoon withdrawal for TRUE composite (Supplementary Fig. S11).

4 Statistical evidence of predictive value of NE_premon

A noticeable NE_{premon} and $CI_{monsoon}$ relation associated with a large-scale driver seeds scope of using NE_{premon} as a predictor of $CI_{monsoon}$. Indeed, in the recent 118

years of IMD rainfall records, 15 out of 19 times NE_{premon} was excess $CI_{monsoon}$ was

non-drought. A toy multiple linear regression model also indicates that NE_{premon} does

have some predictive values. DelSole and Shukla (2002) argued that monsoon seasonal

rainfall is predictable using a linear multiple regression model that uses the ENSO and

Northern Atlantic Oscillation (NAO) indices. They found none as good as the ENSO

index for seasonal monsoon prediction in their regression model. In a similar spirit, we

constructed a toy linear multiple regression model using NE_{premon} and pre-monsoon val-

ues of PDO and ENSO indices. We trained this model on randomly chosen 80% of the

data and tested on the remaining 20%. This regression model could explain 2.46% of $CI_{monsoon}$

when NE_{premon} is included whereas the same model could explain 1.32% of the data with

PDO and ENSO indices alone.

To assess the robustness of our finding, we also checked the statistics of how many

normal $CI_{monsoon}$ years, occurring during joint PDO and ENSO positive phases, were

preceded by normal or excess NE_{premon}. We defined an index as PDO*ENSO (for the

months of March-April-May) to recognize concurrent phases of PDO and ENSO during

the pre-monsoon season and marked more than one standard deviation of this index as

a joint positive state. We identified 18 years with joint positive PDO and ENSO state.

For readers reference, we computed the difference of composite pre-monsoon SST for NE_{premon}

flood and drought years that occurred during these 18 years(Supplementary Fig. S13)

and the results are consistent with the NE_{premon} and SST correlation map depicted in

Fig. 3. Of these 18 years, 14 were normal or above $CI_{monsoon}$ years, and of these 14 years,

12 were normal or above NE_{premon} years.

These statistics emphasize the potential of NE_{premon} as a reliable indicator of $CI_{monsoon}$.

Most importantly, during the joint PDO-ENSO phases, when the threat of extreme drought

monsoon looms over India (enveloped by the 2 ellipses in Figure 2), 92% (12 out of 13)

of the time $CI_{monsoon}$ that followed an excess NE_{premon} was not a drought.

5 Conclusion and Discussions

Climatologically, the Indian monsoon brings about 80% of the total annual rain-

fall over India. However, monsoon strength exhibits considerable interannual variabil-

ity. Some monsoon years are considerably deficit of rainfall or simply droughts. These

drought monsoon years are often associated with the positive phase of ENSO (a.k.a. El

Nino). Since the positive-PDO spatial pattern is similar to a positive-ENSO phase, a joint PDO-ENSO positive phase is argued to drive severe drought monsoons (Krishnamurthy). We found those monsoon years that are exceptions to this are often preceded by excess pre-monsoon rainfall over NE India. A comparative analysis of composites of years with excess NE_{premon} followed by versus not followed by $CI_{monsoon}$ revealed that excess NE_{premon} are produced by the interaction of the large-scale circulation associated with a joint PDO-ENSO positive phase with the complex NE India topography. Further in this composite analysis, a month-wise assessment of the evolution of positive rainfall anomalies over India suggests that a warmer troposphere, a consequence of excess NE_{premon}, drives a stronger monsoon circulation and enhances $CI_{monsoon}$.

We reported a signal that debunks a monsoon drought false alarm. However, we could not elucidate why it is dominant in some years and not in others. The biggest obstacle was to extract a signal for a small region like northeastern India for a multidecadal time scale. Especially because we attempted to isolate northeastern India and central India under this signal. Attempts to design atmospheric modeling experiments to test this mechanism were clouded by the fact that similar initial oceanic forcing, that is, cold sea surface temperature anomalies in the north Pacific, may drive two diverging final states, viz., drought and non-drought monsoon. Systematic biases of climate models in the simulating accurate spatial distribution of Indian monsoon rainfall (Choudhury et al., 2021) was also a restraining factor for conducting modeling experiments, given the small size and geographical location of the northeast Indian region. In addition, current Global Climate Models (GCMs) have systematic biases in simulating diurnal cycles and Katabatic winds. Models precipitate too early in the day (Christopoulos & Schneider, 2021). Coarse spatial resolution and unresolved topography understandably limit climate models' fidelity in simulating the Katabatic winds. Hunt et al. (2022) reported that Ketabatic winds play a critical role in determining convective activity along mountain slopes. Finer resolution and improved understanding of physical processes represented in a model will help design experiments to investigate the mechanism reported in this study further.

We presented compelling statistics establishing a definite connection between NE_{premon} and $CI_{monsoon}$, emphasizing that this connection can be used to identify false alarms of $CI_{monsoon}$ droughts. We also presented a convincing evidence unveiling a mechanism and associated causality explaining this connection. Our finding of utilizing pre-monsoon rainfall over northeastern India as a predictor of monsoon rainfall over central India would

offer critical assistance in the seasonal forecast of monsoon rainfall. Particularly, when the Pacific Ocean exhibits positive phases of PDO and ENSO, the monsoon is expected to be a drought. Such years would be more likely in the coming phase of the PDO (currently, it is in its cold phase), which would expectedly be a warm phase with cold SST anomalies in the northern Pacific and with El Ninos projected to occur more frequently in a warmer climate (Cai et al., 2023).

6 Open Research

The observed rainfall data analyzed in this study are from the IMD (Pai et al., 2015), and Tropical Rainfall Measurement Mission (TRMM) Multi-Satellite Precipitation Analysis (TMPA) 3B42 Version 7 product (Huffman et al., 2007), reanalysis data from 5th generation ECMWF reanalysis product (ERA5) (Hersbach et al., 2023), SST data from the HadISST1 dataset provided by the Met Office Hadley Centre (Rayner, 2003) is available at `https://www.metoffice.gov.uk/hadobs/hadisst/`. The PDO and ENSO indices are taken from (`http://research.jisao.washington.edu/pdo/PDO.latest.txt`) and (`https://psl.noaa.gov/gcos_wgsp/Timeseries/Data/nino34.long.anom.data`), respectively. The linear regression model, that we constructed, is based on the Linear-Regression function from sklearn Python package; the python script for this regression analysis is available at (B. B. Goswami, 2023).

References

Borah, P., Venugopal, V., Sukhatme, J., Muddebihal, P., & Goswami, B. (2020). Indian monsoon derailed by a north atlantic wavetrain. *Science*, *370*(6522), 1335–1338.

Cai, W., Ng, B., Geng, T., Jia, F., Wu, L., Wang, G., . . . others (2023). Anthropogenic impacts on twentieth-century enso variability changes. *Nature Reviews Earth & Environment*, 1–12.

Choudhury, B. A., Rajesh, P., Zahan, Y., & Goswami, B. (2021). Evolution of the indian summer monsoon rainfall simulations from cmip3 to cmip6 models. *Climate Dynamics*, 1–26.

329   Choudhury, B. A., Saha, S. K., Konwar, M., Sujith, K., & Deshamukhya, A.   (2019).

330   Rapid drying of northeast india in the last three decades: Climate change or

331   natural variability?   *Journal of Geophysical Research: Atmospheres*, *124*(1),

332   227-237.   Retrieved from `https://agupubs.onlinelibrary.wiley.com/doi/`

333   `abs/10.1029/2018JD029625`   doi: https://doi.org/10.1029/2018JD029625

334   Christopoulos, C., & Schneider, T. (2021). Assessing biases and climate implications

335   of the diurnal precipitation cycle in climate models.   *Geophysical Research Let-*

336   *ters*, *48*(13), e2021GL093017. doi: https://doi.org/10.1029/2021GL093017

337   DelSole, T., & Shukla, J. (2002). Linear prediction of indian monsoon rainfall. *Jour-*

338   *nal of Climate*, *15*(24), 3645–3658.

339   Douville, H., Raghavan, K., Renwick, J., Allan, R. P., Arias, P. A., Barlow, M., . . .

340   Zolina, O. (2021). Water cycle changes. In V. Masson-Delmotte et al. (Eds.),

341   *Climate change 2021: The physical science basis. contribution of working group*

342   *i to the sixth assessment report of the intergovernmental panel on climate*

343   *change* (chap. 8). Cambridge University Press.

344   Goswami, B. B. (2023). Linear_regression_model (v1.0) [Software]. *Zenodo*. doi: 10

345   .5281/zenodo.8414507

346   Goswami, B. N. (2005). South Asian Summer Monsoon: An overview; in The Global

347   Monsoon System: Research and Forecast.   In *Third International Workshop*

348   *on Monsoon (IWM-III) (2-6 November 2004, Hangzhou, China) (TMRP 70)*

349   *(WMO TD 1266)*

350   Hersbach, H., Bell, B., Berrisford, P., Biavati, G., Horányi, A., Muñoz-Sabater,

351   J., . . . Thépaut, J.-N.   (2023).   ERA5 monthly averaged data on pressure

352   levels from 1940 to present [Dataset]. Copernicus Climate Change Service

353   (C3S) Climate Data Store (CDS).   Retrieved from `https://cds.climate`

354   `.copernicus.eu/cdsapp#!/dataset/10.24381/cds.6860a573?tab=overview`

355   doi: 10.24381/cds.6860a573

356   Huffman, G. J., Bolvin, D. T., Nelkin, E. J., Wolff, D. B., Adler, R. F., Gu, G.,

357   . . . Stocker, E. F.   (2007, 2).   The TRMM Multisatellite Precipitation Anal-

358   ysis (TMPA): Quasi-Global, Multiyear, Combined-Sensor Precipitation Es-

359   timates at Fine Scales.   *Journal of Hydrometeorology*, *8*(1), 38–55.   doi:

360   10.1175/JHM560.1

361   Hunt, K. M. R., Turner, A. G., & Schiemann, R. K. H.   (2022).   Katabatic and

convective processes drive two preferred peaks in the precipitation diurnal cycle over the central himalaya. *Quarterly Journal of the Royal Meteorological Society*, *148*(745), 1731-1751. doi: https://doi.org/10.1002/qj.4275

Krishnamurthy, L., & Krishnamurthy, V. (2014). Decadal scale oscillations and trend in the indian monsoon rainfall. *Climate dynamics*, *43*, 319–331.

Krishnamurthy, V., & Goswami, B. N. (2000). Indian monsoon–enso relationship on interdecadal timescale. *Journal of climate*, *13*(3), 579–595.

Kumar, K. K., Rajagopalan, B., & Cane, M. A. (1999). On the weakening relationship between the indian monsoon and enso. *Science*, *284*(5423), 2156–2159.

Malik, A., Brönnimann, S., Stickler, A., Raible, C. C., Muthers, S., Anet, J., . . . Schmutz, W. (2017). Decadal to multi-decadal scale variability of indian summer monsoon rainfall in the coupled ocean-atmosphere-chemistry climate model socol-mpiom. *Climate dynamics*, *49*, 3551–3572.

Mujumdar, M., Bhaskar, P., Ramarao, M. V. S., Uppara, U., Goswami, M., Borgaonkar, H., . . . Niyogi, D. (2020). Droughts and floods. In R. Krishnan, J. Sanjay, C. Gnanaseelan, M. Mujumdar, A. Kulkarni, & S. Chakraborty (Eds.), *Assessment of climate change over the indian region: A report of the ministry of earth sciences (moes), government of india* (pp. 117–141). Singapore: Springer Singapore. Retrieved from `https://doi.org/10.1007/978-981-15-4327-2_6` doi: 10.1007/978-981-15-4327-2_6

Myers, C. G., Oster, J. L., Sharp, W. D., Bennartz, R., Kelley, N. P., Covey, A. K., & Breitenbach, S. F. (2015). Northeast indian stalagmite records pacific decadal climate change: Implications for moisture transport and drought in india. *Geophysical Research Letters*, *42*(10), 4124-4132. doi: https://doi.org/10.1002/2015GL063826

Pai, D. S., Sridhar, L., Badwaik, M. R., & Rajeevan, M. (2015, 8). *Analysis of the daily rainfall events over India using a new long period (1901–2010) high resolution (0.25° × 0.25°) gridded rainfall data set* (Vol. 45) (dataset No. 3-4). doi: 10.1007/s00382-014-2307-1

Parthasarathy, B. (1995). Monthly and seasonal rainfall series for all india homogeneous regions and meteorological subdivisions: 1871-1994. *Indian Institute of Tropical Meteorology Research Report*, RR–65.

Ray, K., Warsi, A., Bhan, S., & Jaswal, A. (2016). Diurnal variations in rainfall over

indian region using self recording raingauge data. *Current Science*, 682–686.

Rayner, N. A. (2003). Global analyses of sea surface temperature, sea ice, and night marine air temperature since the late nineteenth century. *Journal of Geophysical Research*, *108*(D14). Retrieved from `https://www.metoffice.gov.uk/hadobs/hadisst` doi: 10.1029/2002JD002670

Saha, M., Santara, A., Mitra, P., Chakraborty, A., & Nanjundiah, R. S. (2021). Prediction of the indian summer monsoon using a stacked autoencoder and ensemble regression model. *International Journal of Forecasting*, *37*(1), 58–71.

Shahi, N. K., Rai, S., & Mishra, N. (2019). Recent predictors of indian summer monsoon based on indian and pacific ocean sst. *Meteorology and Atmospheric Physics*, *131*, 525–539.

Sharma, D., Das, S., & Goswami, B. N. (2023). Variability and predictability of the northeast india summer monsoon rainfall. *International Journal of Climatology*, *43*(11), 5248-5268. doi: https://doi.org/10.1002/joc.8144

Singh, D., Ghosh, S., Roxy, M. K., & McDermid, S. (2019). Indian summer monsoon: Extreme events, historical changes, and role of anthropogenic forcings. *Wiley Interdisciplinary Reviews: Climate Change*, *10*(2), e571.

Takaya, Y., Kosaka, Y., Watanabe, M., & Maeda, S. (2021). Skilful predictions of the asian summer monsoon one year ahead. *Nature Communications*, *12*(1), 2094.

Thomas, L., Malap, N., Grabowski, W. W., Dani, K., & Prabha, T. V. (2018). Convective environment in pre-monsoon and monsoon conditions over the indian subcontinent: the impact of surface forcing. *Atmospheric Chemistry and Physics*, *18*(10), 7473–7488. Retrieved from `https://acp.copernicus.org/articles/18/7473/2018/` doi: 10.5194/acp-18-7473-2018

Updated Rainfall Normal based on data of 1971-2020. (2022). *IMD Press Release*. Retrieved from `https://internal.imd.gov.in/press_release/20220414_pr_1572.pdf`

Wang, B., Jin, C., & Liu, J. (2020, 8). Understanding Future Change of Global Monsoons Projected by CMIP6 Models. *Journal of Climate*, *33*(15), 6471–6489. Retrieved from `https://journals.ametsoc.org/doi/10.1175/JCLI-D-19-0993.1` doi: 10.1175/JCLI-D-19-0993.1

Xavier, P., Marzin, C., & Goswami, B. N. (2007). An objective definition of the

428   Indian summer monsoon season and a new perspective on the ENSO-monsoon

429   relationship.   *Quarterly Journal of the Royal Meteorological Society*, *133*(624),

430   749–764. doi: 10.1002/qj

431 Yun, K.-S., & Timmermann, A. (2018). Decadal monsoon-enso relationships reexam-

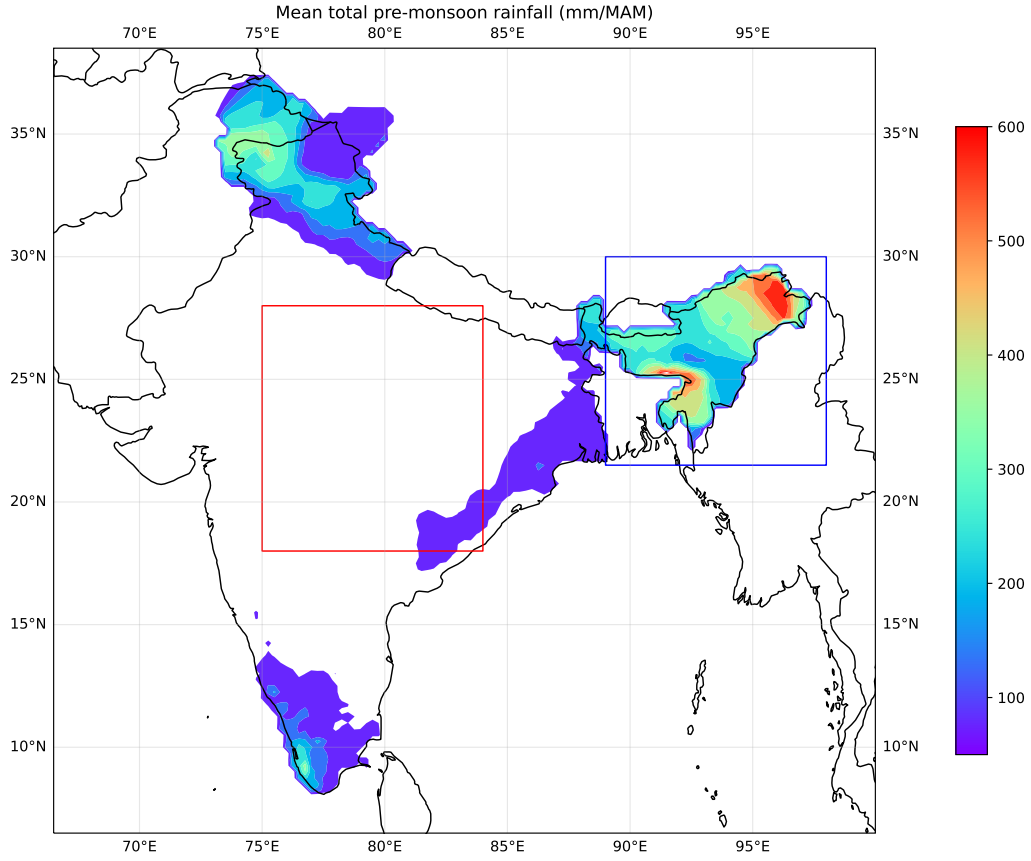432   ined. *Geophysical Research Letters*, *45*(4), 2014–2021.

Figure 1. Mean pre-monsoon (Mar-May) total seasonal rainfall (mm season^{-1}). Central India (CI; indicated by the red box 18°N–28°N, 75°E–84°E). Northeastern India (NE; indicated by the blue box 21.5°N–30°N, 89°E–98°E). The rainfall data is from IMD (1901-2018).
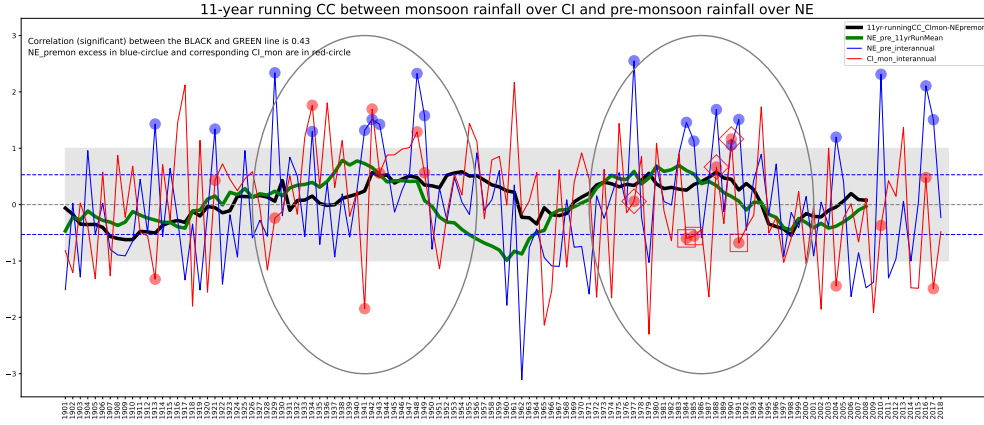
Figure 2. Running correlation and mean. The thick back line indicates 11 year running correlation between $CI_{monsoon}$ and NE_{premon}. The grey dotted line indicates 0 correlation and the blue dotted lines indicate the 90% significant correlation values for N=11. The two ellipses mark the two periods of high correlation between NE_{premon} and $CI_{monsoon}$. The blue and red lines indicate deviations of NE_{premon} and $CI_{monsoon}$, respectively, from their respective long term climatological seasonal means. The green thick line indicates 11-year running means of deviations of NE_{premon} (that is, the blue line). The blue circular markers indicate excess NE_{premon} (excess is defined as more than 1 standard deviation; indicated by the grey shading) and the red circular markers indicate corresponding $CI_{monsoon}$. The rainfall data is from IMD (1901-2018).
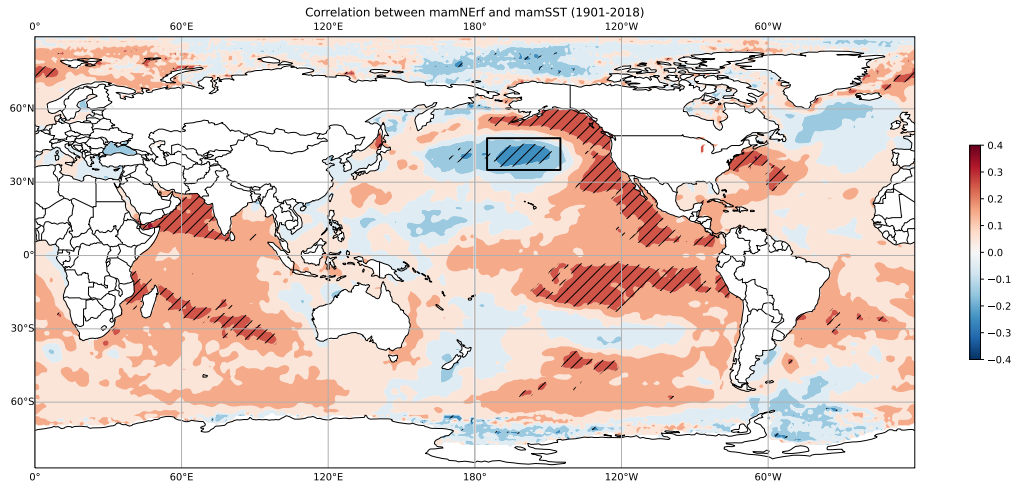
Figure 3. Correlation of NE_{premon} with global SST. Simultaneous correlation of pre-monsoon rainfall over northeastern India with mean SST for the same season. Correlation values above 95% significance level are hatched. The black box indicates region of maximum negative correlation that will be used to compute domain average SST to be used in the Extended Data Figure 6. The rainfall and SST data are from IMD and HadSST, respectively (1901-2018).
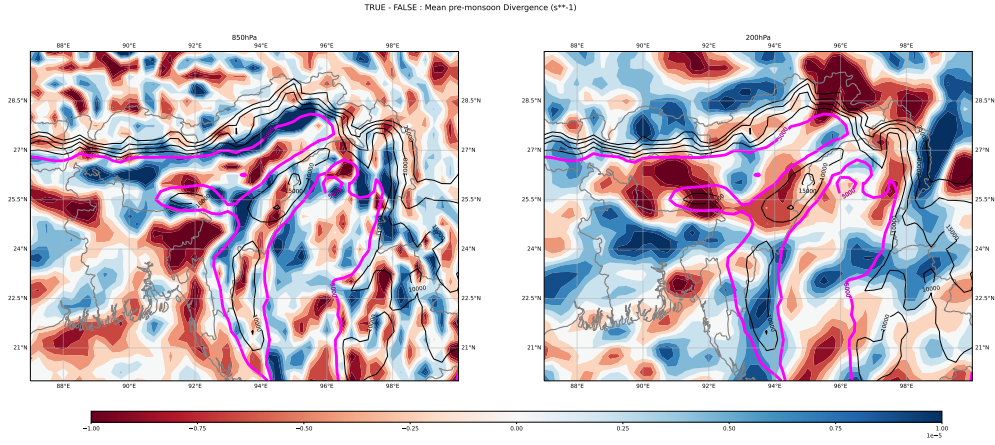
Figure 4. Mean pre-monsoon divergence field for TRUE minus FALSE composite at (a) 850hPa and (b) 200hPa; where TRUE composite is defined as the composite of 3 years (marked by red diamonds in Figure 2) when excess NE_{premon} was followed by above long-term average $CI_{monsoon}$ and FALSE composite is defined as the composite of 3 years (marked by red squares in Figure 2) when excess NE_{premon} was followed by $CI_{monsoon}$ below its long-term average. Black contours indicate geoptential (geopotential=5000 m2/s2 is emphasized in thick magenta contour)) Data source: ERA5.
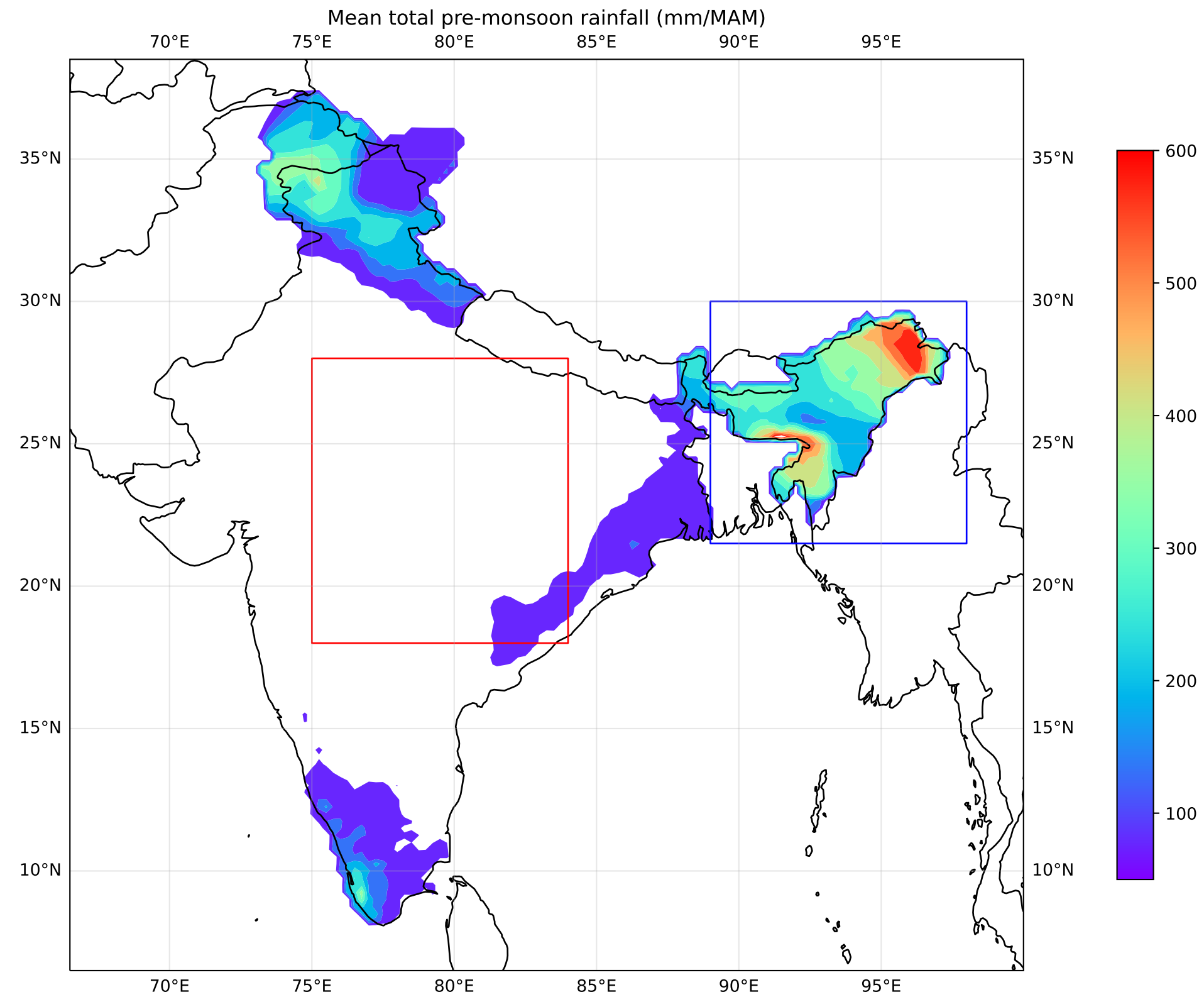
Figure 1.

Mean total pre-monsoon rainfall (mm/MAM)

Figure 2.

11-year running CC between monsoon rainfall over CI and pre-monsoon rainfall over NE

Correlation (significant) between the BLACK and GREEN line is 0.43
NE_premon excess in blue-circlue and corresponding CI_mon are in red-circle

Legend:
- 11yr-runningCC_CImon-NEpremon
- NE_pre_11yrRunMean
- NE_pre_interannual
- CI_mon_interannual

Figure 3.

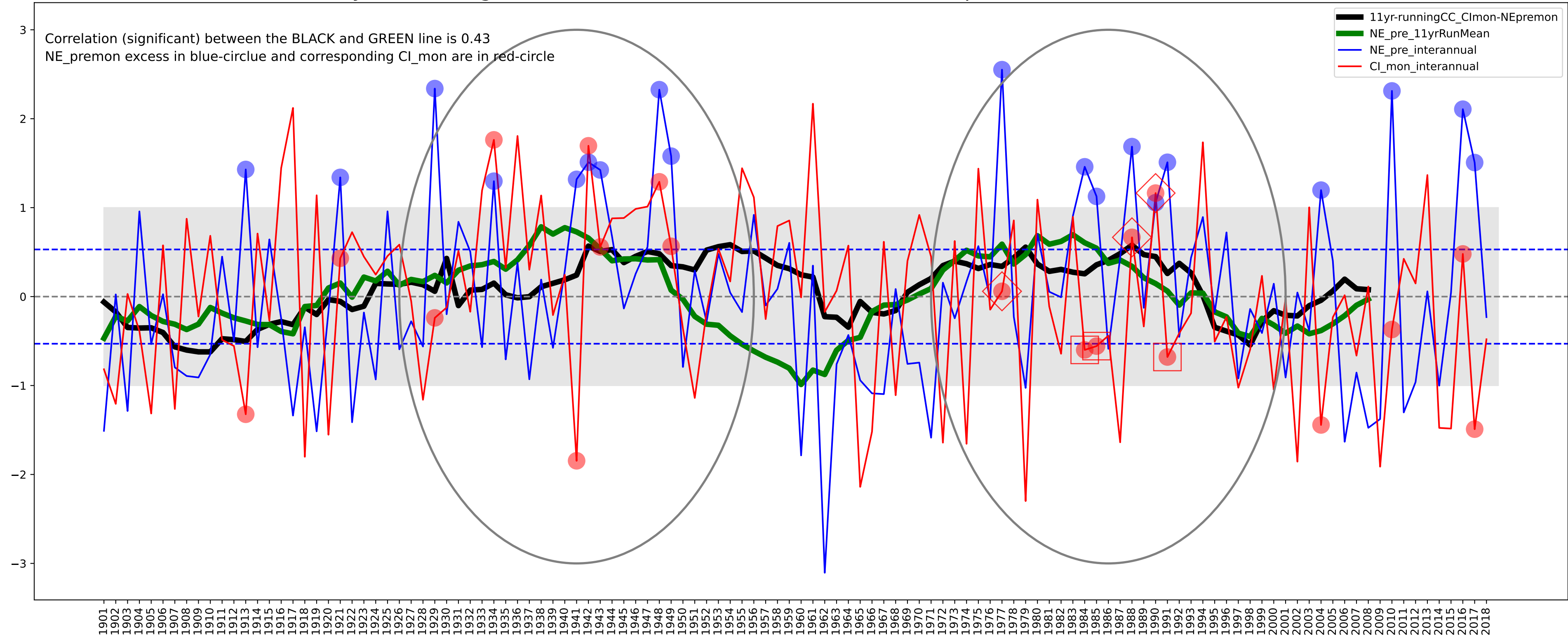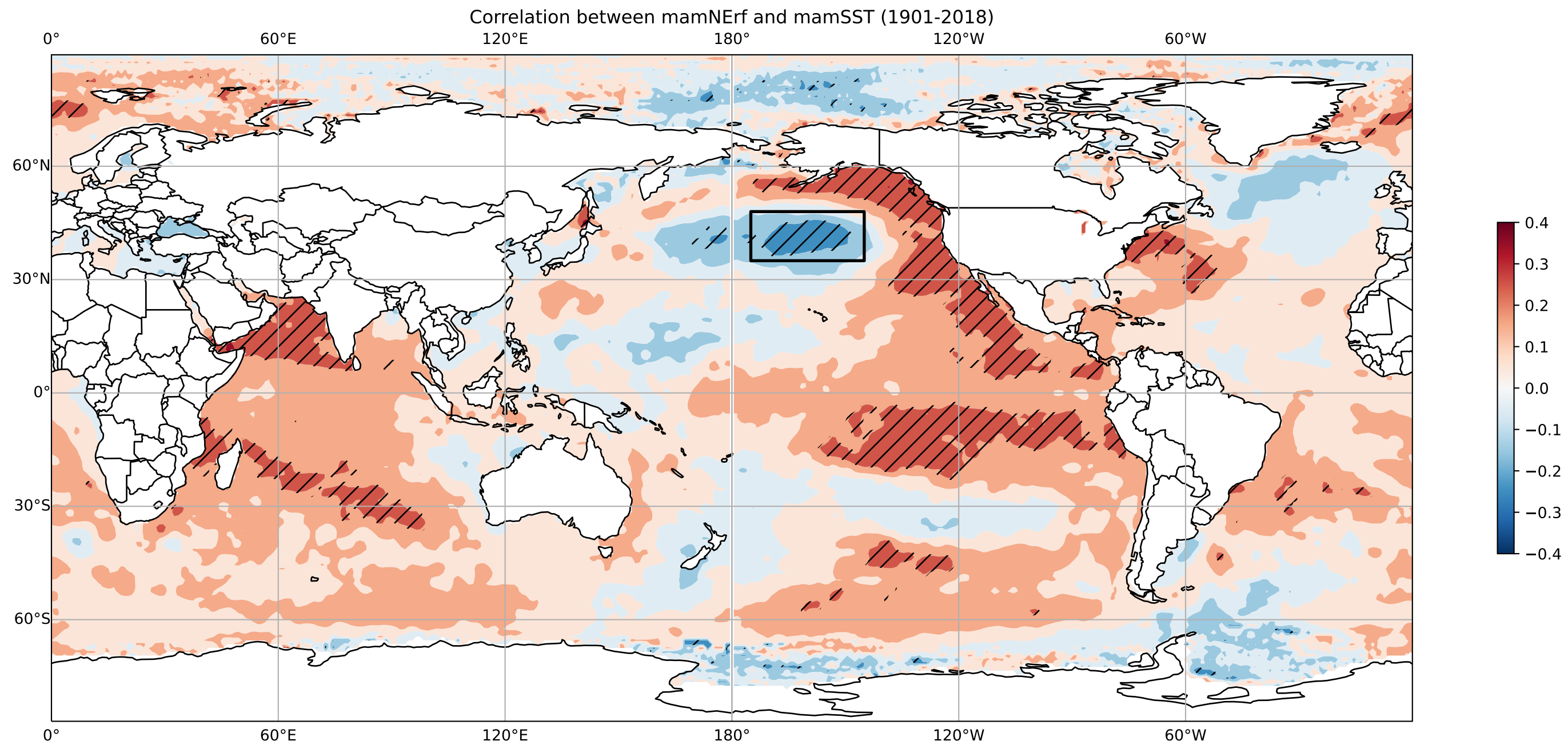Correlation between mamNErf and mamSST (1901-2018)

Figure 4.

TRUE - FALSE : Mean pre-monsoon Divergence (s**-1)